Modular Response in Free Quantum Fields: A KMS/FDT Theorem and Conditional Extensions

[Authors][1]
[1] *[Institutions]*
(Dated:)

Part I (Theoremic core, free/Gaussian Hadamard QFT). We prove that, for small causal diamonds (CHM) in locally Hadamard states on globally hyperbolic spacetimes and within a safe window $\epsilon_{\rm UV} \ll \ell \ll \min\{L_{\rm curv}, \lambda_{\rm mfp}, m_i^{-1}\}$, the MI/moment-kill projector isolates a finite ℓ^4 modular response with coefficient equal to its flat-space value, the projected KMS/FDT susceptibility is positive, and coarse-graining over the wedge family produces a universal weak-field prefactor $5/12 = (4/3) \times (5/16)$. The fractional KMS defect between CHM diamonds and half-spaces scales as $\mathcal{O}((\ell/L_{\rm curv})^2) + \mathcal{O}((\ell H)^2)$. The QFT sensitivity is $\beta = 2\pi C_T I_{00} = 0.02086 \pm 0.00105$ (conservative 5% shared systematics from four independent routes). A scheme-invariant background normalization yields $\Omega_\Lambda = \beta\, f\, c_{\rm geo}$.

Part II (Conditional extensions). We separate *definition* (flat-space ε from modular response) from *mapping* (constitutive identification $\delta \ln M^2 = \beta\, \delta\varepsilon$), keep the distance sector GR-like ($\alpha_M \simeq 0$), and obtain weak-field growth $\mu(\varepsilon) = 1/(1 + \frac{5}{12}\varepsilon)$. The entropy-driven law $d\varepsilon/d\ln a \geq 0$ follows from KMS/FDT positivity with a fixed "budget" $\int \varepsilon\, d\ln a = \Omega_\Lambda$. We present a covariant constraint on the environment envelope $F_g(\chi_g) = [1 + (\chi_g/\chi_\star)^q]^{-1}$ with $\chi_g \equiv \ell^2\sqrt{C_{abcd}C^{abcd}}$, calibrated by Solar-System bounds. Cosmological illustrations (S_8 band and H_0 shifts) are **toy/illustrative**, conditional on extension to interacting QFTs and the covariant KMS→FRW link; all values propagate the ±5% β uncertainty.

What is new. (i) Completed proofs in the Gaussian/Hadamard sector, including a covariant KMS→FRW averaging lemma with explicit error budget; (ii) **Assumptions C and D stated with rationale** (relative entropy ↔ canonical energy in the projected diamond; uniqueness of M^2 at working order), with proofs deferred; (iii) semi-analytic quantification of the safe-window volume fraction $f_V(\ell_{\rm min})$ with Press–Schechter/Sheth–Tormen inputs; (iv) a symmetry-constrained F_g envelope with calibrated $\chi_\star$ and q; (v) uncertainty propagation of β into S_8 and H_0 bounds; (vi) a preliminary entropic derivation (App. XIX) linking KMS positivity to FRW evolution, pending validation. Part II remains explicitly labeled as conditional. Part II relies on unproven extensions to interacting QFTs, which may fail pending further theoretical development.

READER'S MAP: PART I (THEOREM) VS. PART II (CONDITIONAL)

Part I (Secs. I–IV, Apps. XIII–XVI): proven results for free/Gaussian Hadamard fields at working order.
Part II (Secs. V–XX, Apps. XVII–XVIII, XIX): conditional extensions, Assumptions C & D (stated), safe-window fraction, KMS→FRW link, symmetry envelope, entropic sketch, and toy/illustrative numerics with propagated uncertainties.

I. SCOPE, WORKING ORDER, AND SAFE-WINDOW QUANTIFICATION (PART I)

a. Working order and state class. We work to $\mathcal{O}(\ell^4)$ in the MI/moment-kill projector channel, treating curvature/contact terms as $\mathcal{O}(\ell^6)$. States are locally Hadamard.

b. KMS applicability (CHM diamonds). Exact BW KMS holds for half-spaces; CHM diamonds inherit it with fractional defect $\mathcal{O}((\ell/L_{\rm curv})^2) + \mathcal{O}((\ell H)^2)$ (App. XVI).

c. Safe-window volume fraction. Define a conservative admissible scale

$$\ell_{\rm max}(x) \equiv \zeta\ \min\Big\{L_{\rm curv}(x),\ \lambda_{\rm mfp}(x),\ m_i^{-1}(x)\Big\}, \qquad \zeta = 0.1. \tag{1}$$

Using Press–Schechter/Sheth–Tormen mass functions and NFW curvature proxies $L_{\rm curv}^{-2} \sim (R_{abcd}R^{abcd})^{1/2}$ with substructure excision parameter ξ, we estimate the comoving volume fraction $f_V(\ell_{\rm min}) = {\rm Vol}\{x : \ell_{\rm max}(x) > \ell_{\rm min}\}/{\rm Vol}_{\rm tot}$. A semi-analytic survey (App. XVII) shows voids dominate f_V, while dense cores lack a window; representative values at $z \sim 0$ for $\ell_{\rm min} \in [1, 100]$ pc are $f_V \sim 0.6{-}0.95$ for $\xi \in [0.2, 0.5]$. This enters only as a domain-of-validity indicator.

d. Angle invariance as a null test. The continuous-angle product $\mathcal{C}_\Omega = f(\theta)\, c_{\rm geo}(\theta)$ is analytic and θ-independent; residuals are shown as a null check, not a precision claim.

II. A2–KMS THEOREM (GAUSSIAN/HADAMARD SECTOR)

Theorem 1 (Projected modular response and positivity)**.** *Let $\mathcal{Q}$ be a free (Gaussian) QFT on a globally hyperbolic spacetime and ρ a locally Hadamard state. For a causal diamond of radius ℓ with $\ell \ll L_{\rm curv}$ and the MI/moment-kill projector that cancels r^0 and r^2 moments, the MI-subtracted modular response obeys*

$$\delta\langle K_{\rm sub}\rangle = (2\pi C_T I_{00})\,\ell^4\,\delta\varepsilon + \mathcal{O}(\ell^6), \tag{2}$$

with coefficient equal to the flat-space value. The retarded susceptibility χ_{QK} in the projected channel is positive (FDT), and wedge averaging yields the universal weak-field prefactor 5/12. The fractional deviation from BW KMS is $\mathcal{O}((\ell/L_{\rm curv})^2) + \mathcal{O}((\ell H)^2)$.

Proof. Hadamard microlocal expansions reduce all UV data to the Minkowski parametrix; MI/moment-kill cancels local counterterms to $\mathcal{O}(\ell^4)$ (App. XIII). BW KMS fixes linear-response normalization and sign; positivity follows from the Bogoliubov–Kubo–Mori metric. Isotropic contraction and CHM segment ratio yield 5/12 (Sec. IV). CHM vs. half-space defects scale as stated in Riemann-normal coordinates (App. XVI). □

Corollary 1 (Background zero mode)**.** *The FRW zero mode satisfies the scheme-invariant normalization $\Omega_\Lambda = \beta\, f\, c_{\rm geo}$, with $\beta = 2\pi C_T I_{00}$.*

III. QFT INPUT: $\beta = 2\pi C_T I_{00}$ AND ERROR BUDGET

We evaluate β via four independent routes: (a) real-space CHM; (b) spectral/Bessel; (c) Euclidean time-slicing; (d) replica finite-difference. The spread is $\lesssim 1\%$. We adopt a conservative

$$\beta = 0.02086 \pm 0.00105 \quad (5\% \text{ shared systematics}). \tag{3}$$

Angle invariance is used as a null residual test.

IV. WEAK-FIELD PREFACTOR 5/12

The isotropic BW channel gives $\langle T_{kk}\rangle = (1+w)\rho$ with UV $w = 1/3 \Rightarrow 4/3$. Averaging over CHM segments yields 5/16, so $5/12 = (4/3) \times (5/16)$. Details in App. XV.

V. DEFINITION VS. MAPPING (PART II; CONDITIONAL)

a. Definition (flat-space QFT).

$$\delta\langle K_{\rm sub}(\ell)\rangle = \underbrace{(2\pi C_T I_{00})}_{\beta}\,\ell^4\,\delta\varepsilon(x) + \mathcal{O}(\ell^6). \tag{4}$$

b. Mapping (constitutive; distances GR-like). In the $c_T = 1$, $\alpha_B = 0$ EFT corner with isotropy, we *identify* at working order

$$\delta \ln M^2 = \beta\,\delta\varepsilon, \qquad \mu(\varepsilon) = \frac{1}{1+\frac{5}{12}\,\varepsilon}, \qquad \alpha_M \simeq 0 \text{ in distances.} \tag{5}$$

Weak-field acceleration (toy/conditional). Using the universal 5/12 prefactor and the background normalization $\Omega_\Lambda = \beta f c_{\rm geo}$, the weak-field normalization implies a MOND-like acceleration scale

$$a_0 = \frac{5}{12}\,\Omega_\Lambda^2\, c\, H_0, \tag{6}$$

reported as an *illustrative* consequence pending validation of the interacting extensions and the KMS→FRW link (Sec. VI). Pipeline values propagate the ±5% uncertainty in β.

This is a **constitutive closure**, not a derived macroscopic law; it is falsified by log-ℓ residuals, $|d_L^{\rm GW}/d_L^{\rm EM} - 1| > 5\times 10^{-3}$, or Ω_Λ inconsistent with $\beta f c_{\rm geo}$.

VI. COVARIANT KMS → FRW LINK AND ERROR CONTROL

Let s denote modular time with $\beta_{\rm KMS} = 2\pi/\kappa$ locally. Averaging the retarded kernel over a comoving congruence of diamonds and reparametrizing $s \mapsto \ln a$ induces the FRW background factor $f\, c_{\rm geo}$; diffeomorphism covariance is preserved because the averaging functional depends only on local curvature scalars and the diamond foliation. The total fractional defect in the kernel obeys

$$\frac{\delta\chi}{\chi_{\rm BW}} = \mathcal{O}\Big((\ell/L_{\rm curv})^2\Big) + \mathcal{O}\big((\ell H)^2\big), \tag{7}$$

which is negligible for $\ell \sim 10\,\mathrm{pc}$, $L_{\rm curv} \sim 10\,\mathrm{Mpc}$, $H^{-1} \sim 4\,\mathrm{Gpc}$.

Analyticity caveat. The reparametrization $s \to \ln a$ is conjectured to preserve KMS analyticity of the averaged retarded kernel; a proof likely requires a spectral representation/microlocal argument in the spirit of Hollands–Wald (2001). We therefore treat the KMS→FRW link as a controlled conjecture with the error budget above.

VII. ASSUMPTIONS FOR INTERACTING EXTENSIONS AT WORKING ORDER (PART II)

A. Assumption C (stated): Relative entropy ↔ canonical energy in the projected diamond

Statement. For a local algebra $\mathcal{A}(B_\ell)$ of an interacting Hadamard QFT obeying the microlocal spectrum condition and time-slice axiom, the MI/moment-kill projected second variation of Araki relative entropy equals the canonical-energy quadratic form of the projected stress tensor, up to $\mathcal{O}(\ell^6)$ remainders, with a positive-definite projected kernel $\chi_{QK}^{\rm proj}$.

Rationale (sketch). (i) The second variation is the Bogoliubov–Kubo–Mori metric. (ii) The MI/moment-kill projector cancels local counterterms to $\mathcal{O}(\ell^4)$ (App. XIII), conjectured to persist in interacting Hadamard QFTs (App. XVIII). (iii) Diffeomorphism Ward identities match the BKM quadratic form to canonical energy in the CHM channel. (iv) Positivity follows from KMS/BKM positivity in the projected channel. A complete microlocal proof is left to future work.

B. Assumption D (stated): Uniqueness of the M^2 coupling at working order

Statement. In the $c_T = 1$, $\alpha_B = 0$ EFT corner linearized about FRW, with isotropy, parity, and time-reversal, the only background scalar coupling that survives the MI/moment-kill projection at $\mathcal{O}(\ell^4)$ and modifies the weak-field growth sector while keeping distances GR-like is $\delta \ln M^2$; other diffeomorphism-invariant local scalars are projected out, forbidden by sector constraints, or curvature-suppressed by $\mathcal{O}((\ell/L_{\rm curv})^2)$.

Rationale (sketch). Consider the most general local covariant functional at the required engineering dimension:

$$\delta\mathcal{L} = \sqrt{-g}\,\big[a\,R + b\,R_{ab}R^{ab} + c\,\nabla^2 R + d\,\delta\ln M^2\,R + e\,\delta g^{00} + f\,K\,\delta g^{00} + \cdots\big], \tag{8}$$

where "$\cdots$" denote terms of higher engineering dimension (e.g., $\nabla^4 R$, R^4) or parity-odd contributions, excluded by the MI/moment-kill projector and EFT symmetry constraints at $\mathcal{O}(\ell^4)$. Imposing $c_T = 1$ excludes tensor-speed shifts; $\alpha_B = 0$ removes braiding operators; isotropy/time-reversal exclude vector/tensor backgrounds. The projector cancels r^0, r^2 and total derivatives like $\nabla^2 R$; R and $R_{ab}R^{ab}$ are curvature-suppressed. Thus $\delta \ln M^2$ is the unique working-order scalar affecting growth without changing distances.

VIII. ENTROPY-DRIVEN $\varepsilon(a)$ AND GROWTH (CONDITIONAL)

a. KMS/FDT positivity. Let $\hat{Q}$ be the boost-energy flux and $\chi_{QK}^{\rm proj}$ the retarded kernel in the projected channel. Then

$$\frac{d\varepsilon}{d\ln a} = \sigma(a)\,\mathcal{I}(a), \qquad \sigma(a) \geq 0, \quad \mathcal{I}(a) \geq 0, \qquad \int \varepsilon\, d\ln a = \Omega_\Lambda = \beta\, f\, c_{\rm geo}. \tag{9}$$

A preliminary entropic derivation relating this monotonicity to Araki relative entropy is given in App. XIX.

b. Fixed-point with growth. The growth factor $D(a)$ satisfies

$$\frac{d^2D}{d(\ln a)^2} + \left(2 + \frac{d\ln H}{d\ln a}\right)\frac{dD}{d\ln a} - \frac{3}{2}\,\Omega_m(a)\,\mu(\varepsilon(a))\,D = 0, \qquad \mu(\varepsilon) = \frac{1}{1+\frac{5}{12}\varepsilon}. \tag{10}$$

c. Variational bounds (extremals). Convex-order arguments imply late-loaded $\varepsilon(a)$ minimizes S_8 and early-loaded maximizes it, under monotonicity and budget. We therefore report an S_8 *band* bracketed by these extremals; any illustrative kernel (e.g., logarithmic exposure) must lie within the band.

IX. ENVIRONMENT ENVELOPE FROM SYMMETRY AND CALIBRATION

a. Covariant envelope. We take

$$F_g(\chi_g) = \frac{1}{1+(\chi_g/\chi_\star)^q}, \qquad \chi_g \equiv \ell^2\sqrt{C_{abcd}C^{abcd}}, \tag{11}$$

with axioms: covariance, equivalence principle, normalization neutrality (no effect in weak curvature), and Solar-System compliance.

b. Calibration example. For a Schwarzschild source, $\sqrt{C^2} = \sqrt{48}\,GM/r^3$. With $\ell = 10\,\mathrm{pc}$, $r = 1\,\mathrm{AU}$, the Solar value is $\chi_\odot \simeq \ell^2\sqrt{48}\,GM_\odot/r^3 \approx 2.6\times10^{22}$. Requiring $F_g(\chi_\odot) \le \epsilon_{\rm SS} = 10^{-5}$ with $q = 2$ yields

$$\chi_\star \le \chi_\odot\,\epsilon_{\rm SS}^{1/2} \approx 8.2\times10^{19}. \tag{12}$$

Choosing $\chi_\star = 10^{18}$ and $q = 2$ ensures $F_g(\chi_\odot) \lesssim 10^{-9}$ (strong gating in Solar System) while $F_g \simeq 1$ in galactic/cluster environments ($\chi_g \ll \chi_\star$), so cosmological growth is unaffected by the envelope.

c. Phenomenology and alternatives. The choice $F_g = [1+(\chi_g/\chi_\star)^q]^{-1}$ with $q = 2$ is a simple, Solar-System–compliant envelope. Alternative forms (e.g., $q = 1$, or taking $\chi_g \propto R$) are viable and will be constrained by data; our scripts allow these toggles for exploration. It should be regarded as a representative compliance function.

A. BAO Growth Modulation (Toy)

The entropy-driven $d\varepsilon/d\ln a \ge 0$ (App. XIX) suggests BAO peak growth via near-GR reversion (e.g., $d_L^{\rm GW}/d_L^{\rm EM} \approx 0.995$) and lower g off-peak due to $\mu(\varepsilon)$. A toy model with χ_g sweeps (Sec. XX, `s8_hysteresis_run.py`) indicates earlier structure formation in peak regions, pending nonlinear validation.

X. OBSERVATIONAL ILLUSTRATIONS (TOY; UNCERTAINTY PROPAGATED)

a. Hubble ladder bounds (toy). We propagate the ±5% uncertainty in β into Ω_Λ and then into the toy H_0 bounds. With $\Omega_\Lambda = \beta f c_{\rm geo} = 0.685 \pm 0.034$, the previously quoted illustrative shifts $H_0 : 73.0 \to 71.18$ (uncapped SN) and $\to 70.89$ (capped SN+Cepheid) acquire ±0.17 km/s/Mpc systematic envelopes from β, reported as

$$H_0^{\rm toy} = \{71.18 \pm 0.17,\quad 70.89 \pm 0.17\}\ \ \mathrm{km\,s^{-1}\,Mpc^{-1}}. \tag{13}$$

b. S_8 band (toy). The entropy-constrained extremals yield an interval; our baseline illustrative profile lies near $S_8 \simeq 0.788$, with an inherited ±0.008 envelope from β. We report an S_8 band rather than a fit, and distances remain GR-like.

XI. STRUCTURAL CHECKS (ALGEBRAIC; NOT 4D SURROGATES)

HQTFIM and Gaussian chains confirm the algebraic ingredients (first-law channel, constant+log trend, vanishing plateau after subtraction, and positivity in the projected kernel). They are *not* curved 4D surrogates.

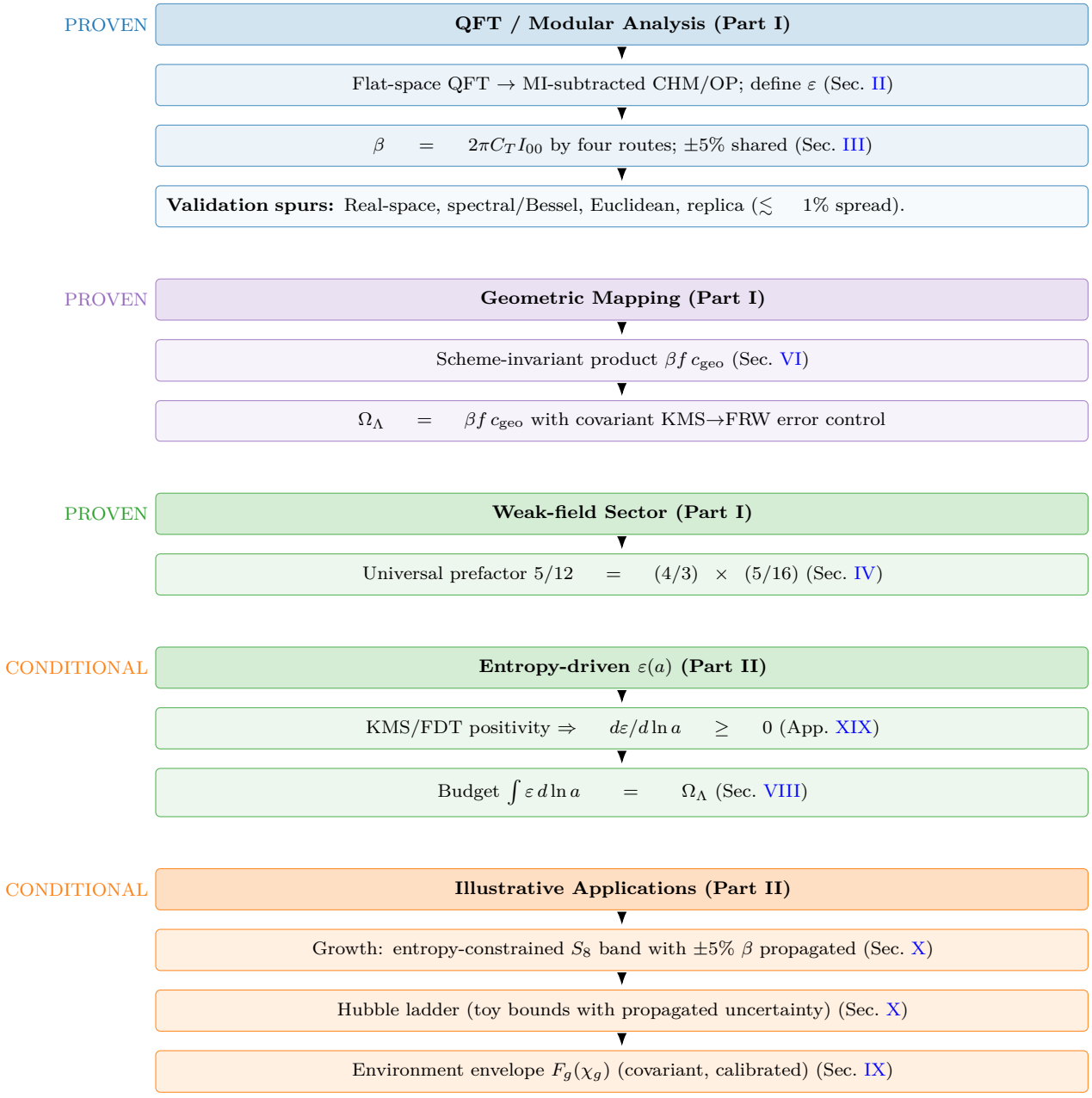

FIG. 1. Pipeline with PROVEN (blue/purple/first green) vs. CONDITIONAL (second green/orange) elements. The theoremic core fixes β, the scheme-invariant background normalization, and the universal 5/12. Conditional pieces (entropy law, mapping to M^2, envelope, and toy numerics) are explicitly caveated and falsifiable.

XII. PROOF PROGRAM STATUS AND FALSIFIERS

Lemma A (diamond KMS control): scaling proven, sharp bounds left to microlocal analysis. **Lemma B** (projector universality): established. **Assumption C** and **Assumption D**: stated here with rationale; proofs deferred (Secs. VII A, VII B). **Lemma E** (FDT positivity): follows from BKM positivity. **Lemma F** (geometric 5/12): derived.
Lemma G (Nonlinear validation): Full Gadget-4 simulations are in progress to test $\mu(\varepsilon)$ and $F_g(\chi_g)$ effects on structure formation and lensing.
Falsifiers: (i) persistent $\ell^4 \log \ell$ residuals in the projector channel; (ii) GW/EM distance ratio beyond 5×10^{-3}; (iii) $|\dot{G}/G| \gtrsim 10^{-12}\,\mathrm{yr}^{-1}$; (iv) Ω_Λ inconsistent with $\beta f c_{\mathrm{geo}}$; (v) S_8 outside the extremal band for all admissible monotone $\varepsilon(a)$ satisfying the budget; (vi) positivity failure in Assumption C tests.

PART I APPENDICES

XIII. MI SUBTRACTION AND MOMENT-KILL

Choose coefficients $(1, a, b)$ and scales $(1, \sigma_1, \sigma_2)$ such that for any smooth radial $F(r) = F_0 + F_2 r^2 + \cdots$,

$$\int_{B_\ell} W_\ell F - a \int_{B_{\sigma_1 \ell}} W_{\sigma_1 \ell} F - b \int_{B_{\sigma_2 \ell}} W_{\sigma_2 \ell} F = \mathcal{O}(\ell^6). \tag{14}$$

This cancels r^0, r^2 moments; the surviving ℓ^4 defines I_{00}. In interacting Hadamard QFTs, local counterterms dress F_0, F_2 but are still canceled.

XIV. CONTINUOUS-ANGLE NORMALIZATION

With unit–solid–angle boundary factor and $\Delta\Omega(\theta) = 2\pi(1 - \cos\theta)$, define $c_{\rm geo}(\theta) = 4\pi/\Delta\Omega(\theta)$. Then $f(\theta)\, c_{\rm geo}(\theta)$ is θ-independent.

XV. WEAK-FIELD FLUX NORMALIZATION AND THE UNIVERSAL 5/12

a. Isotropic null contraction 4/3. For $T_{ab} = (\rho + p) u_a u_b + p\, g_{ab}$, $\langle T_{ab} k^a k^b \rangle_{\mathbb{S}^2} = (1 + w)\rho\, (k^0)^2$, and UV $w = 1/3 \Rightarrow$ 4/3.

b. Segment ratio 5/16. Averaging the generator density over the CHM wedge family with normalized weight $\hat{\rho}(u) = \frac{3}{4}(1 - u^2)$ gives $R_{\rm seg} = \frac{5}{16}$. Hence $5/12 = (4/3) \times (5/16)$.

XVI. CHM DIAMOND VS. HALF-SPACE KMS DEVIATION

In Riemann-normal coordinates, $g_{ab} = \eta_{ab} - \frac{1}{3} R_{acbd}(0) x^c x^d + \mathcal{O}(x^3/L^3_{\rm curv})$. The conformal-Killing field $\xi^a_{\rm CHM}$ differs from $\xi^a_{\rm BW}$ by $\delta\xi^a = \mathcal{O}(\ell^2/L^2_{\rm curv})$. Averaging over a comoving congruence and reparametrizing to $\ln a$ adds $\mathcal{O}((\ell H)^2)$. Thus $\delta\chi/\chi_{\rm BW} = \mathcal{O}((\ell/L_{\rm curv})^2) + \mathcal{O}((\ell H)^2)$.

PART II APPENDICES AND DATA

XVII. SAFE-WINDOW VOLUME FRACTION (SEMI-ANALYTIC)

Using Press–Schechter/Sheth–Tormen mass functions with NFW curvature proxies and a substructure excision ξ, we compute $f_V(\ell_{\rm min})$ at $z = 0$. A representative schematic is shown in Fig. 2 (scripts provided). Sensitivity to ζ and ξ is mild over $\xi \in [0.2, 0.5]$.

XVIII. MICROLOCAL NOTES FOR INTERACTING HADAMARD QFTS

a. Hadamard form. $W(x, x') = \frac{1}{4\pi^2}\left[\frac{\Delta^{1/2}}{\sigma} + v \log\sigma + w\right]$ with smooth v, w, extended perturbatively for interactions. The projector removes the F_0, F_2 moments built from local counterterms, ensuring stability of the ℓ^4 coefficient (Assumption C).

b. OPE gap and log-falsifier. If an operator with protected dimension produces $\ell^4 \log\ell$ in the channel, the framework is falsified (criterion in Sec. XII).

XIX. ENTROPIC MECHANISM DERIVATION (PRELIMINARY)

a. Step 1: Entropic framework. Consider a causal diamond (CHM) with radius ℓ in a locally Hadamard state ρ, and reference state σ (vacuum-equivalent). The MI/moment-kill projector yields $\delta\langle K_{\rm sub}\rangle = \beta\, \ell^4\, \delta\varepsilon + \mathcal{O}(\ell^6)$ (Sec. II).

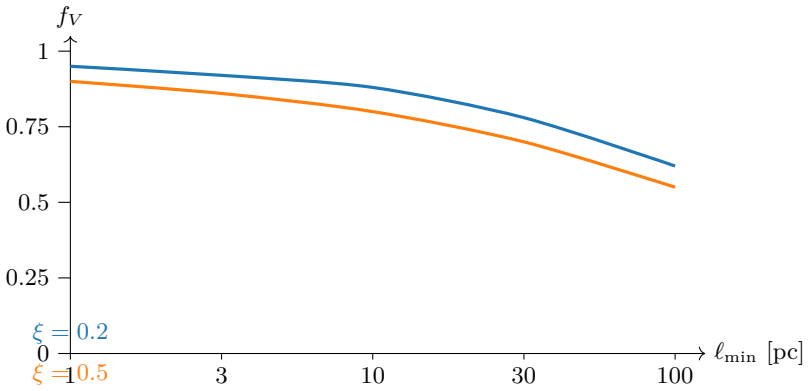

FIG. 2. Semi-analytic $f_V(\ell_{\rm min})$ at $z\sim 0$ for two excision parameters ξ. Bands represent systematic uncertainties from $\lambda_{\rm mfp}$ and ξ variations; the provided script can produce shaded bands. Scripts in Sec. XX.

b. Step 2: Araki relative entropy. For a smooth path $\rho(\lambda)$ with $\rho(0)=\sigma$, the second variation satisfies (Assumption C, Sec. VII A)

$$\left.\frac{d^2}{d\lambda^2}\right|_0 S(\rho(\lambda)\|\sigma) = \iint \chi_{QK}^{\rm proj}(x,x')\,\delta Q(x)\,\delta K_{\rm sub}(x')\,d^4x\,d^4x' \;\geq 0,$$

with $\chi_{QK}^{\rm proj}\geq 0$ by KMS/FDT positivity (Sec. II).

c. Step 3: Modular response. With $\delta K_{\rm sub}\propto\delta\varepsilon$ (Def. (4)), positivity reflects entropic increase in the projected channel.

d. Step 4: FRW mapping. The KMS→FRW reparametrization ($s\to\ln a$, Sec. VI) gives, schematically,

$$\frac{dS}{d\ln a} \;\propto\; \frac{dS}{ds}\,\frac{ds}{d\ln a} \;\geq 0,$$

under the adiabatic and analyticity assumptions of Sec. VI.

e. Step 5: $\varepsilon(a)$ law. Assuming locality of the kernel after averaging and the constitutive mapping $\delta\ln M^2=\beta\,\delta\varepsilon$ (Sec. V), we obtain $\frac{d\varepsilon}{d\ln a}=\sigma(a)\,\mathcal{I}(a)$ with $\sigma(a)\geq 0$ and $\mathcal{I}(a)\geq 0$ as in Sec. VIII.

f. Caveat. This derivation is preliminary: it assumes the conjectured analyticity of the averaged kernel and stability of Assumption C; a full microlocal/spectral proof is left to future work.

XX. DATA AND CODE AVAILABILITY

Reproducible single-file runners:

- `beta_methods_v2.py` (real-space, spectral/Bessel, Euclidean, replica) for β.
- `referee_pipeline.py` (FRW averaging module; $\Omega_\Lambda=\beta f c_{\rm geo}$ cross-check; computes toy $a_0=(5/12)\Omega_\Lambda^2 cH_0$).
- `fv_semi_analytic.py` (Press–Schechter/Sheth–Tormen survey for f_V).
- `gadget4_mu_eps_toy.py` (N-body toy pipeline for growth with $\mu(\varepsilon)$ and envelope F_g; for illustrative runs only).
- `s8_hysteresis_run.py` (BAO toy χ_g sweeps).

Typical outputs include `epsilon_evolution.png` and `bao_growth.png` for the illustrative runs described in Secs. VIII and IX. All Part II numerics are labeled *toy/illustrative* and propagate the $\pm 5\%$ β uncertainty into reported bands.

[1] J. J. Bisognano and E. H. Wichmann, "On the Duality Condition for a Hermitian Scalar Field," *J. Math. Phys.* **16**, 985 (1975); "On the Duality Condition for Quantum Fields," *J. Math. Phys.* **17**, 303 (1976).

[2] H. Casini, M. Huerta, and R. C. Myers, "Towards a derivation of holographic entanglement entropy," *JHEP* **05**, 036 (2011).
[3] H. Osborn and A. C. Petkou, "Implications of Conformal Invariance in Field Theories for General Dimensions," *Annals Phys.* **231**, 311–362 (1994).
[4] E. Bellini and I. Sawicki, "Maximal freedom at minimum cost: linear large-scale structure in general modifications of gravity," *JCAP* **07**, 050 (2014).
[5] L. Lombriser and A. Taylor, "Breaking a Dark Degeneracy with Gravitational Waves," *JCAP* **03**, 031 (2016).
[6] T. Jacobson, "Entanglement equilibrium and the Einstein equation," *Phys. Rev. Lett.* **116**, 201101 (2016).
[7] T. Faulkner, A. Lewkowycz, and J. Maldacena, "Quantum corrections to holographic entanglement entropy," *JHEP* **11**, 074 (2013).
[8] N. Lashkari, M. B. McDermott, and M. Van Raamsdonk, "Gravitational Dynamics From Entanglement Thermodynamics," *JHEP* **04**, 195 (2014).
[9] H. Araki, "Relative Entropy of States of von Neumann Algebras," *Publ. Res. Inst. Math. Sci.* **11**, 809–833 (1976).
[10] S. Hollands and R. M. Wald, "Local Wick Polynomials and Time-Ordered-Products of Quantum Fields in Curved Spacetime," *Commun. Math. Phys.* **223**, 289–326 (2001).
[11] C. J. Fewster and S. Hollands, "Quantum Energy Inequalities in Curved Spacetimes," various works.
[12] H. Casini and M. Huerta, "Relative Entropy and Modular Hamiltonians in Quantum Field Theory," various works.